Electrochimica Acta 54 (2009) 2781–2789

Contents lists available at ScienceDirect

Electrochimica Acta

journal homepage: www.elsevier.com/locate/electacta

Microstructural analysis of the ageing of pseudo-binary (Ti,Zr)Ni intermetallic compounds as negative electrodes of Ni-MH batteries

B. Guiose, F. Cuevas*, B. Décamps, E. Leroy, A. Percheron-Guégan

Equipe de Chimie Métallurgique des Terres Rares, ICMPE, UMR7182, CNRS, 2-8 rue Henri Dunant, 94320 Thiais Cedex, France

ARTICLE INFO

Article history:
Received 8 October 2008
Received in revised form 6 November 2008
Accepted 6 November 2008
Available online 24 November 2008

Keywords:
Ni-MH battery
TiNi
KOH corrosion
Cycle-life
TEM

ABSTRACT

Ageing of $Ti_{1.02-x}Zr_xNi_{0.98}$ ($0 \le x \le 0.48$) compounds during the electrochemical cycling in aqueous KOH electrolyte has been investigated. Microstructural and chemical characterisation, mostly conducted by transmission electron microscopy, show that for all electrodes their activation results from calendar KOH corrosion. After activation, Zr substituted compounds attain much higher capacity (~350 mAh g^{-1}) than the binary TiNi compound (~150 mAh g^{-1}) but their cycle-life is poor. The mechanism of electrode degradation differs for the binary and the substituted compounds. For TiNi, degradation is due to KOH corrosion whereas, for substituted compounds, it mainly results from the loss of electrical contact due to particle pulverisation. For all electrodes, KOH corrosion produces a double surface layer formed by an inner two-phase (Ni–NiO) nanocrystalline layer and an outer $(Ti,Zr)O_2$ amorphous layer.

1. Introduction

TiNi intermetallic compound is known to react with hydrogen both by solid–gas [1] and electrochemical reaction [2–7]. By solid–gas reaction, it absorbs up to 1.4 hydrogen atoms per formula unit (H f.u.$^{-1}$) at normal temperature and pressure. As for electrochemistry, it exhibits a reversible hydrogen capacity of 230 mAh g^{-1} at slow discharging rates with good cycle-life behaviour [3]. Therefore, though its capacity has to be improved for industrial applications, this compound is a promising candidate to be used in nickel-metal hydride (Ni-MH) batteries. Nowadays, the negative electrode of commercial Ni-MH batteries consists of either AB_5 or AB_3 compounds with a typical reversible capacity of 320 mAh g^{-1} and 380 mAh g^{-1}, respectively [8,9].

Several authors have shown that the substitution of Zr for Ti leads to a high increase of the reversible capacity in TiNi-based electrodes [10–12]. Recently, Cuevas et al. have demonstrated that this increase is related to the polymorphic properties of TiNi compound [12–15]. On cooling, the crystal structure of TiNi transforms at 325 K from the high-temperature cubic structure $Pm\bar{3}m$ (B2) into a monoclinic structure $P2_1/m$ (B19′) [16,17]. Since the transformation is martensitic type, the high and low temperature phases are commonly denoted as austenitic and martensitic phases, respectively. Cuevas et al. have shown that, at normal conditions of temperature and hydrogen pressure, $Ti_{0.64}Zr_{0.36}Ni$ compound absorbs 1.6 H f.u.$^{-1}$ and 2.6 H f.u.$^{-1}$ for austenitic and martensitic phases, respectively [13]. Hydrogen is absorbed in the austenitic phase as a solid solution, whereas hydrogen absorption in the martensitic phase occurs through the formation of two hydride phases of composition $Ti_{0.64}Zr_{0.36}NiH$ and $Ti_{0.64}Zr_{0.36}NiH_{2.6}$ [14,15]. When this compound is used as negative electrode of Ni-MH batteries, it exhibits a good reversible capacity for the martensitic phase (330 mAh g^{-1}) but the cycle-life is poor [12].

In view of these results, we have enlarged our research to $Ti_{1.02-x}Zr_xNi_{0.98}$ intermetallic compounds for a wide range of Zr-content ($0 \le x \le 0.48$). In a recent paper [18], we have shown that for the binary compound ($x = 0$), hydrogen is essentially absorbed as a solid solution up to 1.4 H f.u.$^{-1}$. In contrast, for the substituted compounds ($0.12 < x < 0.48$) hydrogen is absorbed up to 2.6 H f.u.$^{-1}$ through the formation of the two hydride phases above reported. Consequently, electrochemical discharge capacities of 150 mAh g^{-1} and 350 mAh g^{-1} have been obtained for the binary and the substituted compounds, respectively.

In this work, the cycle-life of $Ti_{1.02-x}Zr_xNi_{0.98}$ intermetallic compounds as negative electrodes of Ni-MH batteries is presented. A microstructural/chemical analysis by transmission electron microscopy (TEM) of electrode ageing during electrochemical cycling in KOH aqueous solution has been performed. The effect of electrode soaking in KOH has also been studied.

2. Experimental

Ti-rich $Ti_{1.02-x}Zr_xNi_{0.98}$ intermetallic compounds with $x = 0, 0.12, 0.24, 0.36$ and 0.48 have been synthesized as described in Ref. [18].

* Corresponding author. Tel.: +33 1 49 78 12 25; fax: +33 1 49 78 12 03.
E-mail address: cuevas@icmpe.cnrs.fr (F. Cuevas).

0013-4686/$ – see front matter © 2008 Elsevier Ltd. All rights reserved.
doi:10.1016/j.electacta.2008.11.024

Electrochemical experiments were performed at room temperature using a one compartment open cell with the usual 8 M KOH as electrolyte. This electrochemical cell is composed of a negative working-electrode containing $Ti_{1.02-x}Zr_xNi_{0.98}$ hydride powder as active material, a $Ni(OH)_2$/NiOOH counter-electrode, a polyamide insulator inserted between the working and the counter electrodes, and a Hg/HgO reference electrode. The active material was produced by solid–gas hydrogenation of the intermetallic compounds [18]. Hydride powder was sieved under 63 μm and blended under air with conductive carbon and polytetrafluoroethylene (PTFE) in the weight ratio 90:5:5. The preparation was then rolled down to a thickness of 250 μm and compressed on Ni grids. Electrochemical cycling experiments were performed in galvanostatic mode using a MacPile II device from Bio Logic at a regime of C/10. The cut-off potential was fixed at −0.7 V vs. Hg/HgO.

To establish whether the aqueous electrolyte plays a significant role on the electrode cycle-life, a particular electrode ($Ti_{0.66}Zr_{0.36}Ni_{0.98}$) was also cycled at a lower KOH concentration (6 M). Additionally, the same compound was cycled at 6 M KOH after being soaked in concentrated alkaline solution (8 M KOH) for 72 h. Such a soaking time corresponds to the activation period of the electrode on cycling at 8 M KOH.

The morphologic state of the electrodes before and after cycling was studied by scanning electron microscopy (SEM) using a FEG-LEO 1530 device operated at 15 kV. The electrodes were first embedded in Epoxy resin. Then, the samples were mechanically polished using SiC paper with lessening grain sizes (800, 1200 and 4000 mesh) and ¼ μm-size abrasive diamond paste. Finally a thin layer of Pd/Pt was evaporated on the sample surface to avoid charge effects. SEM backscattered electron micrographs were analysed with an image processing software (ImageJ) to quantify phase contents [19].

The active material powder was mechanically removed from the electrodes at different stages of electrochemical cycling to be analysed by TEM techniques. To study the sole effect of the electrolyte on calendar corrosion, i.e. time-dependent corrosion upon exposure to KOH aqueous electrolyte, microstructural analyses were also performed for $Ti_{0.90}Zr_{0.12}Ni_{0.98}$ electrode after its immersion for 20 days in 8 M KOH at room temperature. TEM experiments were undertaken using a Tecnai F20 with field emission gun operated at 200 kV. Scanning transmission electron microscopy (STEM) in either bright-field or dark-field modes allowed us to characterize the morphological state of the samples. The chemical composition was analyzed using both energy dispersive X-ray (EDX) and electron energy loss spectroscopy (EELS). The crystal structure was also studied by electron diffraction. In order to obtain thin enough samples to be electron transparent and to preserve their surface state, two techniques were used to prepare the samples. The first one consisted in mixing the active material with aluminium powder (20 μm in particle size) and then to put the preparation into a galvanised steel sheet of 0.6 mm. The whole is then rolled down to a thickness lower than 130 μm. Discs of 3 mm diameter were then punched out and thinned down to perforation using an ion polisher (precision ion polishing system, PIPS). The second technique used was ultramicrotomy. Powder active material was embedded in epoxy resin and then cut by a diamond knife into thin slices (100–150 nm). The slices were then deposited on a carbon coated copper grid.

3. Results and discussion

3.1. Cycle-life

Fig. 1 displays the electrochemical discharge capacity as a function of the number of cycles for the $Ti_{1.02-x}Zr_xNi_{0.98}$ ($0 \le x \le 0.48$) compounds cycled in 8 M KOH. Cycle-life curves can be split in two parts: a first one, named activation period, where the discharge capacity increases until the maximum capacity is reached, and a second one, named degradation period, where the discharge capacity decreases. Cycle-life differs for binary and substituted compounds. For the $Ti_{1.02}Ni_{0.98}$ binary compound, the activation is very fast: the maximum capacity, C_{max} = 150 mAh g^{-1}, is reached at the second cycle (Fig. 1). The electrochemical discharge capacity is poor but this electrode shows slow degradation (40% capacity decrease in 100 cycles). On the other hand, the maximum capacity for the substituted compounds is much higher, $C_{max} \sim 350$ mAh g^{-1}, but their cycle-life is very short (the capacity decreases to 90% in around 30 cycles). The activation period lengthens with the increase of Zr-content. In fact, the activation period is very short for $Ti_{1.02-x}Zr_xNi_{0.98}$ compounds with $x < 0.36$ as the maximum capacity is reached at the first cycle. In contrast, the activation period lasts four cycles for $x = 0.36$ and 28 cycles for $x = 0.48$, respectively. Moreover, the electrodes with the faster activation also show the faster degradation (Table 1). The maximum discharge capacities are in close agreement with solid–gas PCI measurements [18].

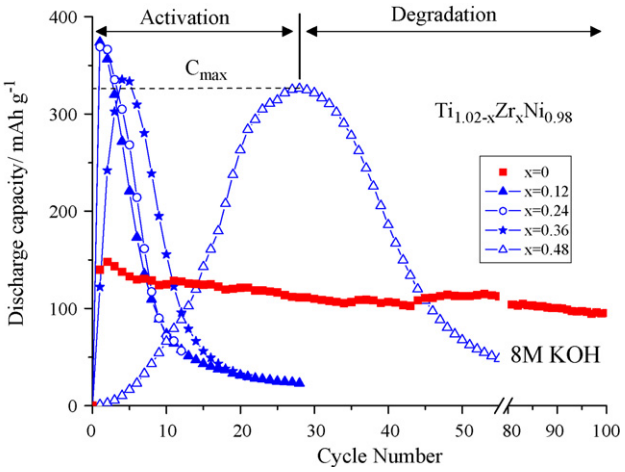

Fig. 1. Cycle-life behaviour of $Ti_{1.02-x}Zr_xNi_{0.98}$ ($0 \le x \le 0.48$) compounds. Activation and degradation periods as well as the maximum discharge capacity, C_{max}, are expressly indicated for $x = 0.48$.

In order to understand the different cycle-life behaviour of these compounds, we have focused our analysis on three electrodes, the binary compound and two substituted compounds, $x = 0.12$ and 0.36, which exhibit distinct but representative cycle-life behaviour. The $Ti_{0.90}Zr_{0.12}Ni_{0.98}$ is activated at the first cycle and then shows fast degradation, whereas the $Ti_{0.66}Zr_{0.36}Ni_{0.98}$ compound, containing three times more Zr, requires longer activation (four cycles) before degradation (Fig. 1 and Table 1).

3.2. Effects of KOH concentration and soaking pre-treatment on the electrochemical cycling

To get a preliminary information on the electrolyte role on the activation and degradation phenomena, two different sets of electrochemical experiments were performed for $x = 0.36$. In the first set, the cycle-life of this electrode was measured either at 6 M or

Table 1
Electrochemical cycle-life properties of $Ti_{1.02-x}Zr_xNi_{0.98}$ ($0 \le x \le 0.48$) compounds.

x	Activation period (cycles)	C_{max} (mAh g^{-1})	Degradation rate at $C_{max/2}$ (mAh g^{-1} per cycle)
0	2	150	–
0.12	1	373	43
0.24	1	369	48
0.36	4	335	36
0.48	28	326	18